MIXED-MODE RESISTANCE CURVE BEHAVIOR OF STRUCTURAL ADHESIVELY BONDED JOINTS

K. M. LIECHTI AND J. H. SHAH

Engineering Fracture Mechanics Laboratory
Department of Aerospace Engineering and Engineering Mechanics
The University of Texas at Austin
Austin, Texas 78712, USA

ABSTRACT

The mixed-mode fracture resistance of an epoxy and a polyurethane adhesive that were used to join composite adherends made of randomly swirled glass fibers in a polyester matrix was considered. Both adhesives gave rise to joint toughness values that increased with increasing shear component. They both also exhibited resistance curve behavior at all mode-mixes. In the case of the epoxy, there was a combination of fiber bridging and inelastic effects as the cracks grew along a subinterfacial path in the composite that paralleled the interface. Crack growth in the composite/urethane joints was entirely adhesive and the resistance curve effect was attributed solely to inelastic effects in the urethane. Finite element analyses that allowed for quasi-static growth of cracks by modeling the interface as a separate constitutive entity supported the observations and shielding mechanisms described above.

KEYWORDS

Adhesive fracture, resistance curve, mixed-mode, shielding.

INTRODUCTION

The motivation for the work described here comes from the automotive industry where relatively low cost, polymer matrix components must be joined by polymeric adhesives in structural joints of primary, load bearing structures. Although the long term durability of such joints must clearly be a concern given the polymeric nature of the components and their relatively low glass transition, the focus of this study has been the resistance to fracture under relatively short term, mixed-mode loading.

A combined experimental/numerical approach was taken. In the experiments, laminated beams were subjected to various fracture mode-mixed using the loading rig proposed by Fernlund and Spelt (1994). Crack tip location and, in some cases, crack tip displacement fields were measured in conjunction with the applied displacements and associated load levels. The quasi-static growth of the cracks was analyzed using finite element methods where different crack paths were modeled by cohesive zones whose characteristics were adjusted to yield the measured load deflection response.

EXPERIMENTS

The adherends were a random swirl glass fiber mat in a polyester matrix. The material was supplied by Dow Chemical under the designation DOW MM 364. Two adhesives were carried throughout the study: an epoxy and a urethane, provided by Goodrich and Ashland companies, respectively. The fracture behavior of joints bonded in this way was examined by making use of laminated beams that were cut from laminated plates. Based on the toughness of the neat adhesive and the strength of the composite, it was found that the thickness of the adherends needed to be greater than 0.7 inches (17.8 mm) in order to prevent yielding or failure in the adherends. The thickness of the composite adherends therefore was chosen to be 0.75 in. (19.1 mm). Nominal adhesive thickness of 0.03 inches/ 0.01 inches (0.076cm/0.025cm) were selected for this work.

The loads F_1 and F_2 applied to the upper and lower adherends of the laminated beams were produced by the mechanism shown in Figure 1, following the work of Fernlund and Spelt (1994). The jig is connected to the servo hydraulic testing machine at the locations A and B and the distances s_1, s_2, s_3 and s_4 are adjusted in order to produce different values of F_1 and F_2.

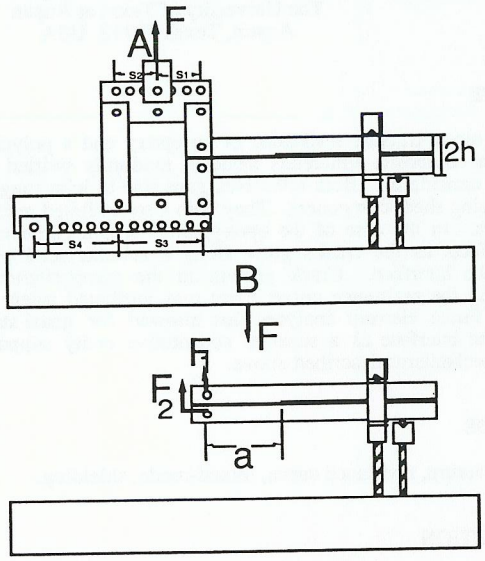

Figure 1. Mixed Mode Fracture Loading Jig.

$$F_1 = F\left(1-\frac{s_1}{s_2}\right) \qquad F_2 = F_1\frac{s_1}{s_2}\left(\frac{1}{1+\frac{s_3}{s_4}}\right) \tag{1}$$

The energy release rate G and fracture mode-mix ψ are then given by

$$G = \frac{6F_1^2a^2}{E_1h^3}\left[1+\left(\frac{F_2}{F_1}\right)^2-\frac{1}{8}\left(1+\left(\frac{F_2}{F_1}\right)^2\right)\right] \tag{2}$$

$$\psi = \tan^{-1}\left[\frac{\sqrt{3}}{2}\frac{\left(\frac{F_1}{F_2}+1\right)}{\left(\frac{F_1}{F_2}-1\right)}\right] \tag{3}$$

The values of energy release rate and fracture mode-mix given in (3) and (4) are the global values (in the sense of Fleck et al. (1991)) which do not account for the presence of the adhesive layer. The corresponding local values of stress intensity factor $K_{loc.}$ and fracture mode-mix ψ_{loc} that account for the presence of the adhesive layer with modulus E_2 and its thickness h_2 can be obtained from

$$K_{loc} = \left(\frac{1-\alpha}{1+\alpha}\right)^{1/2}K^{\infty}e^{i\varphi(c/h_2,\alpha,\beta)} \tag{5}$$

$$\psi_{loc} = \psi + \varphi(c/h_2,\alpha,\beta) \tag{6}$$

where

$$\varphi = \varepsilon\ln\left(\frac{h_2}{c}-1\right)+2\left(\frac{c}{h}-\frac{1}{2}\right)\tilde{\varphi}(\alpha,\beta) \tag{7}$$

The degree of control over the relative values of F_1 and F_2 afforded by this arrangement is much greater than previous schemes. It provides many more intermediate mode-mixes in addition to pure modes I and II. Furthermore, the range of crack lengths over which crack growth is stable is increased by this apparatus (Spelt and Fernlund, 1994). This is particularly true for the mode II (end-notched flexure) condition.

In all experiments, a chevron notch was cut in the adhesive layer and an initial crack was obtained by fatigue loading. The testing machine displacement was applied in a ramp mode at 0.0025 cm/s and the load and the load-line displacement (measured by a DCDT displacement transducer) were recorded on a computerized data acquisition system. A scale was placed on the specimen and a microscope was used to measure the crack length.

Composite/Urethane Specimens

The toughness values of the composite urethane interface under various mixed-mode conditions are plotted in Figure 2. The number in the parenthesis indicates how many data points were used to obtain the average for each mode-mix condition. The most brittle condition for the composite/urethane specimens was under mode I loading, where the toughness value was about 526 N/m (3.0 lb./in). The toughest was the mode II condition, where the toughness reached an average value of 4033 N/m (23 lb./in). In all cases, the composite/urethane specimens failed adhesively. The spread in the data for each mode-mix was due to the fact that the cracks appeared to toughen as they became longer. This effect was most noticeable under mode II conditions where inelastic mechanisms were probably most dominant. Since there was no fiber bridging here, the increase in toughness with mode-mix was most likely also associated with inelastic effects.

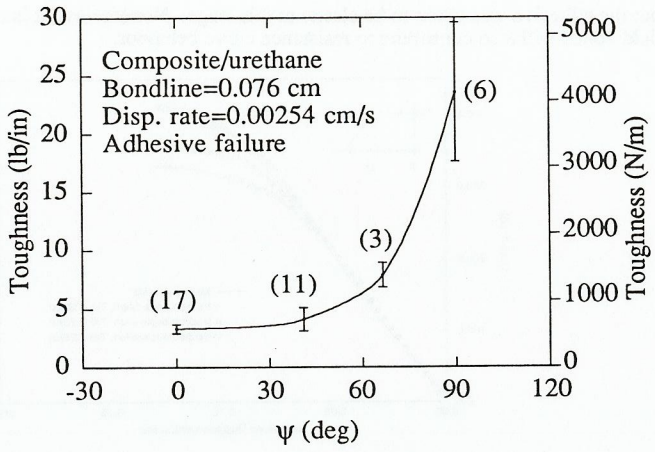

Figure 2. Fracture toughness of composite/urethane specimens as a function of mode-mix.

Composite/Epoxy Specimens

The mixed-mode fracture jig was also used to conduct the composite/epoxy fracture experiments using the same procedures as were employed for the composite/urethane specimens. The bondline thickness was 0.010" and the experiments were conducted at a displacement rate of 0.0025 in/s. The failure mode for this specimen was cohesive in the composite adherend, with the crack running in the adherend in a sub interfacial location parallel to the interface. There was evidence of fiber bridging across the crack faces as the cracks propagated. This indicated that the bonding between the epoxy and the composite adherends was already at its optimal condition from the mechanical point of view. However, not all the composite/epoxy specimens had pure cohesive failure, that is, adhesive failure did sometimes occur, resulting in lower toughness values. The load/displacement response was more elastic than that of the composite/urethane specimens. This was due to the fact that the epoxy is more elastic than the urethane at room temperature.

The toughness values for composite/epoxy specimens under different mode-mix conditions are plotted in Figure 3. The distribution was again U-shaped, but was somewhat flatter than that of the composite/urethane. The toughness had an average value of 1052 N/m (6.0 lb./in) under mode I and 3857 N/m (22.0 lb./in) under mode II. For comparison, the mode I toughness of the neat epoxy was higher (1400 N/m or 8 lb./in). The lower mode I toughness of the joint reflected the lower toughness of the adherends along the sub interfacial layer. Even when the joint toughness exceeded that of the neat adhesive, the crack remained trapped in the sub interfacial zone of the adherends. The spread in the data about the average was again due to resistance curve behavior that resulted from fiber bridging and pullout across the crack faces.

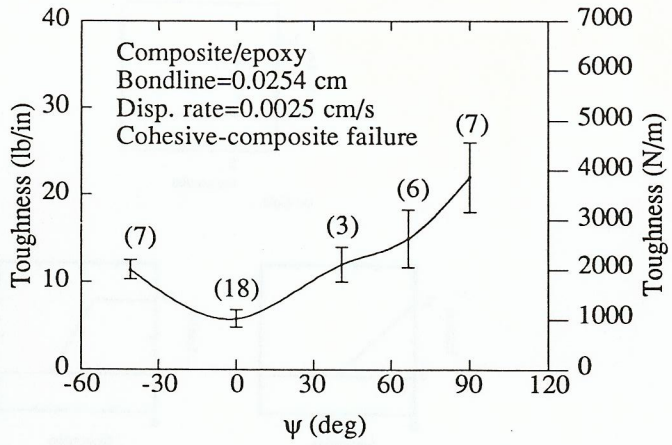

Figure 3. Fracture toughness of composite/epoxy specimens as a function of mode-mix

MODELING OF QUASI-STATIC CRACK GROWTH

The resistance curve behavior that has been noted in the previously described experiments occurred in a quasi static manner. This was further investigated with more detailed measurements of crack growth history and analyses of slowly growing cracks. Modeling of crack growth allows the dissipation associated with inelastic effects and fiber bridging to be determined. Such models require a crack growth criterion to be implemented. This could be as simple as specifying the maximum stress or crack opening displacement that can be accommodated by the material or interface. Cohesive zone models have also been considered and have recently been applied to interfacial crack growth problems (Needleman, 1990 and Tvergaard and Hutchinson, 1994).

Three traction separation laws were considered in this work. The first (Fig. 4) was a rigid separation law. Although this approach was successful in predicting crack initiation loads, it did not capture the resistance curve behavior. Trapezoidal and triangular traction separation laws (Fig. 4) were therefore also considered. With these laws, the area under the traction vs. separation curve represents the intrinsic adhesion of the interface. Tvergaard and Hutchinson (1994) have shown that the area under the curve and the maximum traction are the controlling parameters in these models.

After several refinements, a very fine mesh size of 6,992 nodes and 6,576 four node bilinear plane strain elements was used. A mesh having elements near the crack tip that were 0.0127 cm thick with an aspect ratio of 7 converged to a consistent solution. The crack was made to grow along the adhesive-composite interface. The epoxy was modeled as an isotropic elastic material and the composite as anisotropic elastic using the properties obtained in previous mechanical testing.

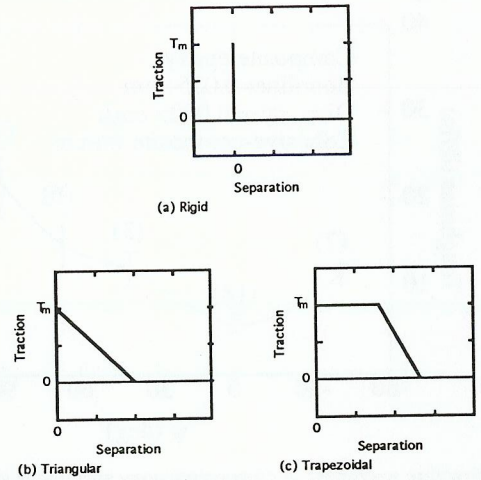

Figure 4. Schematics of traction separation laws.

The rigid separation law did not give rise to the resistance curve behavior that was observed in the experiments . Once the separation traction was reached, the load dropped off with increasing load line displacement, which was not the case in the experiments. The triangular and trapezoidal separation laws gave the same results as long as the energy under their traction separation curves remained the same. Hence, all subsequent finite element analyses were conducted using the trapezoidal separation law unless otherwise specified.

Mode I Fracture

The comparison between finite element analysis and experiment for a specimen under mode I loading is shown in Fig. 5. The measured and predicted stiffness values matched very well and part of the resistance curve behavior was also captured. The best agreement for crack initiation was obtained for a separation traction T_m = 193 MPa (28 ksi). However, none of the models captured the drop in load. In fact, when allowed to continue beyond the load line displacements shown, the load level remained constant. The drop in load level that is a feature of the measured resistance curves will most likely be better modeled once the epoxy nonlinear behavior is incorporated into the model. The plot of measured load as a function of crack length also compared best for a separation traction, T_m = 193 MPa (28 ksi). The measured value of energy release rate for initiation was 263 N/m (1.5 lb./in), rising to a maximum value of 403N/m (2.3 lb./in). This was also captured by the analysis for T_m = 193 MPa (28 ksi) .

The size of the yield zone in the adhesive layer was also of interest. The von Mises stress contour levels at the maximum load indicated that some damage was created in the adherends, possibly explaining some of the fiber bridging that has been observed in the sub interfacial zone. The yield zone in the adhesive layer extended to about eight adhesive layer thickness ahead of the crack tip. This is probably smaller than the actual size due to the fact

that the adhesive was taken to be elastic at this stage. Nonetheless, it is clear that such large yield zones will also contribute to resistance curve behavior.

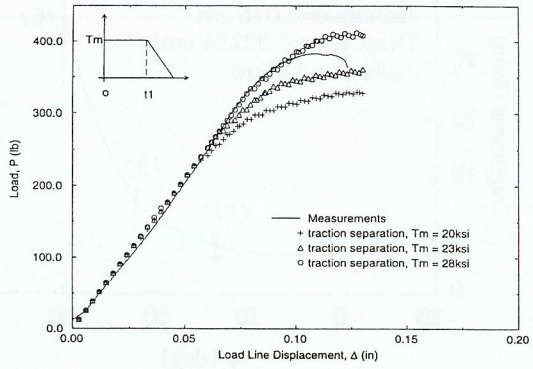

Figure 5. Measured and predicted load displacement response of composite/epoxy specimens under mode I loading

Mixed-Mode Fracture

Experimental and finite element results were also compared for a composite/epoxy specimen under a mixed mode loading (ψ = 40.9°). This is essentially the mixed-mode flexure condition where the lower adherend is free at the left end. Figure 6 compares the plot of the load on the upper adherend as a function of the crack opening displacement for different values of the separation traction (T_m) with the experimental result. The measured response stiffened prior to crack extension, which appears to be an artifact of the loading device. Steel shims had to be inserted under the supports at the right hand end of the specimen in order to avoid crushing. The shims also brought the measured and predicted displacement values into the level of agreement shown. Prior to that, the discrepancy was great. The crack ran in a sub interfacial zone in the adherends parallel to the interface. Plots of load and energy release rate were obtained as a function of crack extension for different values of the traction-separation law. The value T_m = 69 MPa (10 ksi) exhibited the best agreement with the experiments. This is of course different from the value (28 ksi) that gave best agreement under mode I. This suggests that the intrinsic toughness was higher in mode I as opposed to being independent of the mode mix. However, the locus of failure differed in the two cases.

A plot of the von Mises equivalent stress around the crack tip at the maximum loads revealed a failure zone in the composite that was about four times the thickness of the epoxy adhesive. The yield zone in the adhesive was about twenty-five times the adhesive layer thickness. Even with the lower separation traction value, this is about three times larger than the size of the yield zone under mode I conditions, thereby explaining the higher toughness values at a mode mix of 40.9°, which were also noted earlier (Fig. 3). The yield zone size increased with increasing crack length as would be expected for resistance curve behavior. Thus inelastic effects and fiber bridging probably both contribute to the toughening effect.

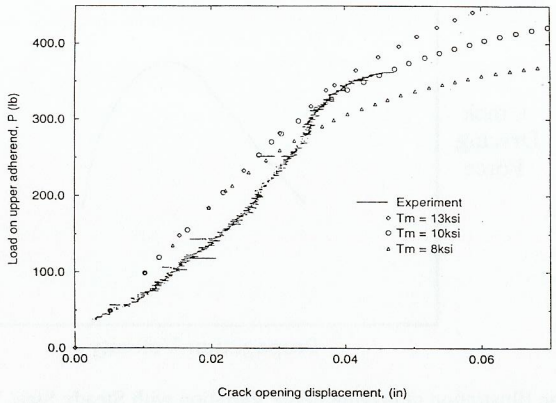

Figure 6. Measured and predicted load displacement response of composite/epoxy specimens under mixed-mode loading ($\psi = 40.9^{o}$).

A similar set of experiments and analyses are underway for the composite/urethane specimens. The urethane has been characterized as a nonlinearly viscoelastic material, which will have to be accounted for in the analysis.

CONCLUSIONS

The fracture toughness of composite/urethane and composite/epoxy joints was a strong function of the fracture mode-mix. During the experiments, there was evidence of resistance curve behavior. The composite/epoxy interface was modeled as a separate constitutive entity in finite element analyses that allowed the crack to grow along the interface. The measured and predicted load displacement behavior matched reasonably well. The analyses indicated that inelastic effects and fiber bridging were responsible for the resistance behavior.

REFERENCES

Fernlund, G. and Spelt, J.K. (1994) Mixed-mode fracture characterization of adhesive joints, Composites Science and Technology, **50**, 441-449.

Fleck N. A., Hutchinson J. W., Suo Z., "Crack path selection in a brittle adhesive layer," *Int. Journal of Solids and Structures* **27** (1991) 1683-1703.

Needleman, A. (1990). An analysis of tensile decohesion along an interface. *Journal of the Mechanics and Physics of Solids* **38**, 289-324.

Tvergaard, V. and Hutchinson, J. W. (1994) Toughness of an interface along a thin ductile layer joining elastic solids. *Phil. Mag. A* **70**, 641-656.